Engineering Notes

Space Structure Vibration Suppression Using Control Moment Gyroscope Null Motion

Jitang Guo*
Harbin Institute of Technology, 150080 Harbin, People's Republic of China
Christopher J. Damaren†
University of Toronto, Toronto, Ontario M3H 5T6, Canada
and
Yunhai Geng‡
Harbin Institute of Technology, 150080 Harbin, People's Republic of China

DOI: 10.2514/1.G004344

I. Introduction

FOR modern spacecraft, possession of large flexible structures can result in vibration during attitude maneuvers, which can have a great impact on attitude control performance. The kinds of actuators that have been applied to vibration suppression [1–3] include the single-gimbaled control moment gyroscope (SGCMG) because of its high torque capacity and moderate interaction with the elastic structure [4].

D'Eleuterio and Hughes [5,6] introduced the concept of a gyroelastic body, referring to an elastic body comprising infinitesimal angular momentum devices, which results in coupled modes, shifted frequencies, and controllable damping. The dynamics of an elastic truss arm with a scissored pair of SGCMGs was examined by Yang et al. [7], who showed that SGCMGs could be used for vibration control. A Lyapunov-based controller was investigated by Shi and Damaren [8] for active damping of a cantilevered beam with a SGCMG and an angular velocity sensor. The collocation of a SGCMG with an angular rate sensor is a strategy that will be employed in the present work. The optimal distribution of control moment gyroscopes on an elastic beam and an elastic plate has been studied [9–11]. These works inform the current Note in terms of suggesting where to locate SGCMGs on the flexible plate, which is studied here. A set of control moment gyroscopes was distributed on the elastic structure of a flexible spacecraft to provide control torques and modal forces for attitude control and vibration suppression in Ref. [12]. A modal force compensator was applied in Ref. [13] to reduce vibration during attitude maneuvers by means of canceling out the disturbance input to the elastic dynamics. However, the methods in Refs. [12,13] require as many SGCMGs as the number of the modes selected to describe the elastic motion, which is satisfied only when using a distribution of many SGCMGs. It should also be emphasized that additional actuators (possibly more SGCMGs or reaction wheels) are required for the attitude control function in those works. In the present Note, the number of SGCMGs can be as little as four, and this arrangement can provide attitude control as well vibration suppression (active damping) of all controllable modes. This is a significant improvement.

It is believed that singularity prevents SGCMGs from being widely applied to attitude control, and considerable progress in singularity avoidance has been made. At a singularity, gimbaled motion results in no net torque. Margulies and Aubrun [14] investigated null motion, and they analyzed the possibility of singularity avoidance for a general SGCMG system. Based on a perturbed matrix theory, Wie [15] proposed a generalized singularity robust (GSR) steering law to drive the control moment gyroscope system to escape from internal singular surfaces. Torque singular states and modal force singular states have been defined and visualized to demonstrate singularity by Hu et al. [16] with a scissored pair of SGCMGs and pyramid-type SGCMGs as examples.

A large flexible spacecraft is considered in this Note, which is viewed as an unconstrained plate with SGCMGs mounted on the elastic structure as actuators. A simple controller based on a Lyapunov function and a GSR steering law incorporating proper null motion are presented to realize the desired attitude maneuver and vibration suppression. It is important to realize that, although null motion produces no net torque, it can produce modal forces on the vibration modes. The proposed method requires at least four SGCMGs to control the attitude and all of the considered vibration modes. A modal analysis is applied to the gyroelastic system with consideration of the proposed method. The effectiveness of the proposed method is demonstrated by attitude maneuver examples using numerical simulations.

II. System Description

The considered system includes an unconstrained elastic plate and a set of SGCMGs, as shown in Fig. 1. The equations of the rotational and elastic dynamics for the system are given by [13]

$$\boldsymbol{J}\dot{\boldsymbol{\omega}} + \boldsymbol{\omega}\times\boldsymbol{J}\boldsymbol{\omega} + \boldsymbol{M}\ddot{\boldsymbol{\tau}} + h_0\sum_{i=1}^{n}\boldsymbol{\omega}\times\boldsymbol{h}_i + h_0\sum_{i=1}^{n}\dot{\boldsymbol{\beta}}_i\times\boldsymbol{h}_i = \boldsymbol{u}_r + \boldsymbol{T}_d \tag{1}$$

$$\boldsymbol{M}^T\dot{\boldsymbol{\omega}} + \ddot{\boldsymbol{\tau}} + \boldsymbol{\Xi}\dot{\boldsymbol{\tau}} + \boldsymbol{K}\boldsymbol{\tau} - h_0\sum_{i=1}^{n}\boldsymbol{R}_i^T\boldsymbol{h}_i\times(\boldsymbol{\omega}+\dot{\boldsymbol{\beta}}_i) = \boldsymbol{u}_e \tag{2}$$

where $\boldsymbol{\omega}$ denotes the angular velocity of a nominal body-fixed frame relative to inertial space, and $\boldsymbol{\tau}$ denotes the generalized coordinate vector for the elastic deflection; $\boldsymbol{J}$ and $\boldsymbol{M}$ represent the moment of inertia of the system and the modal angular momentum matrix, respectively. The external disturbance is $\boldsymbol{T}_d$, and the magnitude of the angular momentum of each SGCMG is h_0. The number of the considered vibration modes is m, and the number of SGCMGs satisfies $n \geq 4$. The symbol $\boldsymbol{\Xi} = \mathrm{diag}\{2\xi_i\omega_i\}$, $i = 1, 2, \ldots, m$, represents the damping matrix and $\boldsymbol{K} = \mathrm{diag}\{\omega_i^2\}$ denotes the stiffness matrix; ω_i and ξ_i represent natural frequencies and the corresponding damping coefficients, respectively. It is important to note that a set of orthogonal constrained modes have been used for spatial discretization, i.e., the elastic modes of the nongyric flexible structure with cantilevered boundary conditions at the mass center.

Received 18 January 2019; revision received 3 May 2019; accepted for publication 22 June 2019; published online 29 July 2019.

*Ph.D. Candidate, Research Center of Satellite Technology; currently Visiting Student, Institute for Aerospace Studies, University of Toronto, Toronto, Ontario M3H 5T6, Canada; guojitang@hit.edu.cn.

†Professor, Institute for Aerospace Studies; damaren@utias.utoronto.ca. Associate Fellow AIAA (Corresponding Author).

‡Professor, Research Center of Satellite Technology; gengyh@hit.edu.cn.

The rotational displacement of the node where the ith SGCMG is mounted is $\boldsymbol{\beta}_i = \boldsymbol{R}_i \boldsymbol{\tau}$, $i = 1, 2, \ldots, n$; and $\boldsymbol{R}_i$ represents the rotational modal matrices (the curl of the mode shapes), which can be obtained from the constrained modes of the structure.

The quantities representing the control torques and modal forces generated by the SGCMG system can be expressed as

$$\boldsymbol{u}_r = \boldsymbol{A}_r \dot{\boldsymbol{\delta}}, \qquad \boldsymbol{u}_e = \boldsymbol{A}_e \dot{\boldsymbol{\delta}} \tag{3}$$

where $\boldsymbol{\delta} = [\delta_1 \quad \delta_2 \quad \cdots \quad \delta_n]^T$ denotes the gimbal angle vector, and $\boldsymbol{A}_r$ and $\boldsymbol{A}_e$ represent Jacobian matrices expressed as

$$\begin{aligned} \boldsymbol{A}_r &= -h_0[\boldsymbol{t}_1 \quad \boldsymbol{t}_2 \quad \cdots \quad \boldsymbol{t}_n] \\ \boldsymbol{A}_e &= -h_0[\boldsymbol{R}_1^T \boldsymbol{t}_1 \quad \boldsymbol{R}_2^T \boldsymbol{t}_2 \quad \cdots \quad \boldsymbol{R}_n^T \boldsymbol{t}_n] \end{aligned} \tag{4}$$

where $\boldsymbol{t}_i = \boldsymbol{g}_i \times \boldsymbol{h}_i$, $i = 1.2, \ldots, n$, represents the opposite direction of the output torque; $\boldsymbol{g}_i$ denotes the gimbal axis vectors; and $\boldsymbol{h}_i$ denotes the unit angular momentum vectors, as shown in Fig. 1.

III. Controller Design

Because the kinematics and dynamics of a flexible spacecraft with SGCMGs have been established, this section will consider controller design to realize the desired attitude maneuver and vibration suppression. Equations (1) and (2) can be combined to give

$$\begin{bmatrix} \boldsymbol{J} & \boldsymbol{M} \\ \boldsymbol{M}^T & \boldsymbol{I} \end{bmatrix} \begin{bmatrix} \dot{\boldsymbol{\omega}} \\ \ddot{\boldsymbol{\tau}} \end{bmatrix} + \begin{bmatrix} \boldsymbol{G}_{rr} & \boldsymbol{G}_{re} \\ -\boldsymbol{G}_{re}^T & \boldsymbol{G}_{ee} + \boldsymbol{\Xi} \end{bmatrix} \begin{bmatrix} \boldsymbol{\omega} \\ \dot{\boldsymbol{\tau}} \end{bmatrix} + \begin{bmatrix} \boldsymbol{0} & \boldsymbol{0} \\ \boldsymbol{0} & \boldsymbol{K} \end{bmatrix} \begin{bmatrix} \boldsymbol{\theta} \\ \boldsymbol{\tau} \end{bmatrix} = \begin{bmatrix} \boldsymbol{u}_r - \boldsymbol{\omega}^\times \boldsymbol{J} \boldsymbol{\omega} \\ \boldsymbol{u}_e \end{bmatrix} \tag{5}$$

where $\boldsymbol{G}_{rr} = -h_0 \sum_{i=1}^{n} \boldsymbol{h}_i^\times$ and $\boldsymbol{G}_{ee} = -h_0 \sum_{i=1}^{n} \boldsymbol{R}_i \boldsymbol{h}_i^\times \boldsymbol{R}_i$ are skew-symmetric matrices: $\boldsymbol{G}_{re} = -h_0 \sum_{i=1}^{n} \boldsymbol{h}_i^\times \boldsymbol{R}_i$ and $\boldsymbol{\theta}$ is defined such that $\dot{\boldsymbol{\theta}} = \boldsymbol{\omega}$. The symbol $\boldsymbol{\omega}^\times$ returns the skew-symmetric matrix

$$\boldsymbol{\omega}^\times = \begin{bmatrix} 0 & -\omega_3 & \omega_2 \\ \omega_3 & 0 & -\omega_1 \\ -\omega_2 & \omega_1 & 0 \end{bmatrix} \tag{6}$$

Rewriting Eq. (5), it follows that

$$\bar{\boldsymbol{M}} \ddot{\boldsymbol{p}} + (\bar{\boldsymbol{G}} + \bar{\boldsymbol{\Xi}}) \dot{\boldsymbol{p}} + \bar{\boldsymbol{K}} \boldsymbol{p} = \boldsymbol{f} \tag{7}$$

where

$$\begin{aligned} &\bar{\boldsymbol{M}} = \begin{bmatrix} \boldsymbol{J} & \boldsymbol{M} \\ \boldsymbol{M}^T & \boldsymbol{I} \end{bmatrix}, \quad \bar{\boldsymbol{G}} = \begin{bmatrix} \boldsymbol{G}_{rr} & \boldsymbol{G}_{re} \\ -\boldsymbol{G}_{re}^T & \boldsymbol{G}_{ee} \end{bmatrix}, \quad \bar{\boldsymbol{\Xi}} = \begin{bmatrix} \boldsymbol{0} & \boldsymbol{0} \\ \boldsymbol{0} & \boldsymbol{\Xi} \end{bmatrix}, \\ &\bar{\boldsymbol{K}} = \begin{bmatrix} \boldsymbol{0} & \boldsymbol{0} \\ \boldsymbol{0} & \boldsymbol{K} \end{bmatrix}, \quad \boldsymbol{p} = \begin{bmatrix} \boldsymbol{\theta} \\ \boldsymbol{\tau} \end{bmatrix}, \quad \boldsymbol{f} = \begin{bmatrix} \boldsymbol{u}_r - \boldsymbol{\omega}^\times \boldsymbol{J} \boldsymbol{\omega} \\ \boldsymbol{u}_e \end{bmatrix} \end{aligned} \tag{8}$$

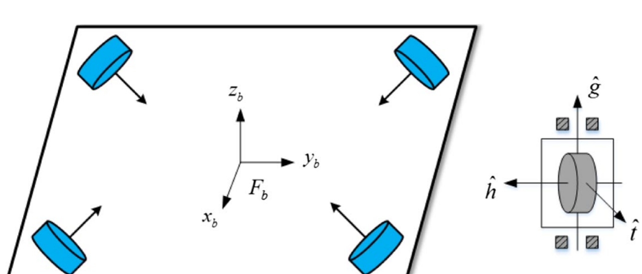

Fig. 1 Model of flexible spacecraft with SGCMGs.

Four quaternions (Euler parameters) are used to express the attitude kinematics as follows:

$$\begin{bmatrix} \dot{q}_0 \\ \dot{\boldsymbol{q}} \end{bmatrix} = \frac{1}{2} \begin{bmatrix} \boldsymbol{q}^T \\ q_0 \boldsymbol{I}_3 + \boldsymbol{q}^\times \end{bmatrix} \boldsymbol{\omega} \tag{9}$$

where $q_0 = \cos(\Theta/2)$, $\boldsymbol{q} = [q_1 \quad q_2 \quad q_3]^T = \boldsymbol{e} \sin(\Theta/2)$, and Θ denotes the rotation angle about the Euler axis $\boldsymbol{e}$.

To realize the desired attitude maneuver and vibration suppression, the following Lyapunov function is chosen:

$$V = k_p[(q_0 - 1)^2 + \boldsymbol{q}^T \boldsymbol{q}] + \frac{1}{2} \dot{\boldsymbol{p}}^T \bar{\boldsymbol{M}} \dot{\boldsymbol{p}} + \frac{1}{2} \boldsymbol{p}^T \bar{\boldsymbol{K}} \boldsymbol{p} \geq 0 \tag{10}$$

where k_p is a positive scalar. The time derivative of V can be written as

$$\begin{aligned} \dot{V} &= k_p \boldsymbol{q}^T \boldsymbol{\omega} + \dot{\boldsymbol{p}}^T (\bar{\boldsymbol{M}} \ddot{\boldsymbol{p}} + \bar{\boldsymbol{K}} \boldsymbol{p}) \\ &= k_p \boldsymbol{q}^T \boldsymbol{\omega} + \dot{\boldsymbol{p}}^T [-(\bar{\boldsymbol{G}} + \bar{\boldsymbol{\Xi}}) \dot{\boldsymbol{p}} + \boldsymbol{f}] \\ &= k_p \boldsymbol{q}^T \boldsymbol{\omega} - \dot{\boldsymbol{\tau}}^T \boldsymbol{\Xi} \dot{\boldsymbol{\tau}} + \boldsymbol{\omega}^T (\boldsymbol{u}_r - \boldsymbol{\omega}^\times \boldsymbol{J} \boldsymbol{\omega}) + \dot{\boldsymbol{\tau}}^T \boldsymbol{u}_e \end{aligned} \tag{11}$$

where $\dot{\boldsymbol{p}}^T \bar{\boldsymbol{G}} \dot{\boldsymbol{p}} = 0$ is used because $\bar{\boldsymbol{G}}$ is a skew-symmetric matrix.

The attitude controller is selected as a proportional-derivative form:

$$\boldsymbol{u}_r = -k_p \boldsymbol{q} - k_d \boldsymbol{\omega} + \boldsymbol{\omega}^\times \boldsymbol{J} \boldsymbol{\omega} \tag{12}$$

where k_d is a positive scalar. Then, the modal force can be calculated by Eq. (3) so that Eq. (11) can be rewritten as

$$\dot{V} = -k_d \boldsymbol{\omega}^T \boldsymbol{\omega} - \dot{\boldsymbol{\tau}}^T \boldsymbol{\Xi} \dot{\boldsymbol{\tau}} + \boldsymbol{b}^T \dot{\boldsymbol{\delta}} \tag{13}$$

where $\boldsymbol{b} = \boldsymbol{A}_e^T \dot{\boldsymbol{\tau}}$ can be expressed using $\dot{\boldsymbol{\beta}}_i$ as

$$\boldsymbol{b} = -h_0 [\dot{\boldsymbol{\beta}}_1^T \boldsymbol{t}_1 \quad \dot{\boldsymbol{\beta}}_2^T \boldsymbol{t}_2 \quad \cdots \quad \dot{\boldsymbol{\beta}}_n^T \boldsymbol{t}_n]^T \tag{14}$$

Because Eq. (13) depends on the steering law of the SGCMG system, it is necessary to design a feasible steering law to satisfy the condition of stabilization, which will be analyzed in the next section.

IV. Steering Law Design

In this section, the steering law of the SGCMG system is developed to satisfy the constraints on the gimbal rates. According to the controller design and stabilization analysis, the constraints on the gimbal rate $\dot{\boldsymbol{\delta}}$ are summarized as follows:

$$\begin{aligned} &\boldsymbol{A}_r \dot{\boldsymbol{\delta}} = \boldsymbol{u}_r \\ &\boldsymbol{b}^T \dot{\boldsymbol{\delta}} \leq 0 \end{aligned} \tag{15}$$

where the first one is the control torque constraint, and the other one is a stabilization constraint designed to render $\dot{V} \leq 0$ in Eq. (13).

Because $n \geq 4$, the Jacobian matrix A_r can be decomposed as

$$\boldsymbol{A}_r = [\boldsymbol{u}_1 \quad \boldsymbol{u}_2 \quad \boldsymbol{u}_3] \begin{bmatrix} \sigma_1 & 0 & 0 & 0 & \cdots & 0 \\ 0 & \sigma_2 & 0 & 0 & \cdots & 0 \\ 0 & 0 & \sigma_3 & 0 & \cdots & 0 \end{bmatrix} \begin{bmatrix} \boldsymbol{v}_1^T \\ \boldsymbol{v}_2^T \\ \vdots \\ \boldsymbol{v}_n^T \end{bmatrix} \tag{16}$$

where σ_i denotes the ith singular value, $\boldsymbol{u}_i$ denotes the ith basis vector of the three-dimensional angular momentum space, and $\boldsymbol{v}_i$ denotes the ith basis vector of the n-dimensional gimbal angle space. In a nonsingular state, only the first three of the $\boldsymbol{v}_i$ can lead to a net control torque. The gimbal rate vector can be divided into two parts as follows:

$$\dot{\boldsymbol{\delta}} = \dot{\boldsymbol{\delta}}_T + \dot{\boldsymbol{\delta}}_N \tag{17}$$

where $\dot{\boldsymbol{\delta}}_T$ represents the gimbal rate vector that generates a net control torque; and $\dot{\boldsymbol{\delta}}_N$ represents the gimbal rate vector satisfying $\boldsymbol{A}_r\dot{\boldsymbol{\delta}}_N = \boldsymbol{0}$, which is referred to as null motion. They can be obtained using

$$\dot{\boldsymbol{\delta}}_T = \boldsymbol{V}_T\boldsymbol{a}_T, \qquad \dot{\boldsymbol{\delta}}_N = \boldsymbol{V}_N\boldsymbol{a}_N \tag{18}$$

where $\boldsymbol{a}_T \in \mathbb{R}^3$, $\boldsymbol{a}_N \in \mathbb{R}^{n-3}$, $\boldsymbol{V}_T = [\,\boldsymbol{v}_1 \quad \boldsymbol{v}_2 \quad \boldsymbol{v}_3\,] \in \mathbb{R}^{n\times 3}$ denotes the tangent space, and $\boldsymbol{V}_N = [\,\boldsymbol{v}_4 \quad \cdots \quad \boldsymbol{v}_n\,] \in \mathbb{R}^{n\times(n-3)}$ denotes the null space. Substituting Eqs. (17) and (18) into Eq. (15) yields

$$\begin{gathered}\boldsymbol{A}_r\dot{\boldsymbol{\delta}}_T = \boldsymbol{u}_r \\ \boldsymbol{b}^T\dot{\boldsymbol{\delta}}_T + \boldsymbol{b}^T\boldsymbol{V}_N\boldsymbol{a}_N \le 0\end{gathered} \tag{19}$$

The control torque constraint can be solved by the pseudoinverse as follows:

$$\dot{\boldsymbol{\delta}}_T = \boldsymbol{A}_r^T(\boldsymbol{A}_r\boldsymbol{A}_r^T)^{-1}\boldsymbol{u}_r \tag{20}$$

which is the minimum two-norm solution without null motion. To satisfy Eq. (19), we would like to select $\boldsymbol{a}_N$ so as to reduce $\boldsymbol{b}^T\dot{\boldsymbol{\delta}}_T + \boldsymbol{b}^T\boldsymbol{V}_N\boldsymbol{a}_N$ to $-\boldsymbol{b}^T\boldsymbol{Q}\boldsymbol{b}$ with $\boldsymbol{Q} = \boldsymbol{Q}^T \ge \boldsymbol{0}$. Thus, the $\dot{\boldsymbol{\delta}}_T$ needs to be cancelled out and $-\boldsymbol{b}^T\boldsymbol{Q}\boldsymbol{b}$ added. To this end, we select

$$\boldsymbol{a}_N = -\boldsymbol{V}_N^T\boldsymbol{b}(\boldsymbol{b}^T\boldsymbol{V}_N\boldsymbol{V}_N^T\boldsymbol{b})^{-1}(\boldsymbol{b}^T\dot{\boldsymbol{\delta}}_T + \boldsymbol{b}^T\boldsymbol{Q}\boldsymbol{b}) \tag{21}$$

The effect of the null motion is to eliminate the effect of $\dot{\boldsymbol{\delta}}_T$ on the elastic dynamics and add proper damping to the system at the same time. Numerical experience has indicated that a suitable choice for $\boldsymbol{Q}$ is $k_N\boldsymbol{V}_N\boldsymbol{V}_N^T$ with $k_N > 0$ (the simpler choice of $\boldsymbol{Q} = k_N\boldsymbol{I}$ did not perform as well in simulation). Then, the steering law can be obtained by combining Eqs. (17), (18), (20), and (21) to give

$$\begin{aligned}\dot{\boldsymbol{\delta}} = {}& \boldsymbol{A}_r^T(\boldsymbol{A}_r\boldsymbol{A}_r^T)^{-1}\boldsymbol{u}_r - \boldsymbol{V}_N\boldsymbol{V}_N^T\boldsymbol{b}(\boldsymbol{b}^T\boldsymbol{V}_N\boldsymbol{V}_N^T\boldsymbol{b})^{-1}[\boldsymbol{b}^T\boldsymbol{A}_r^T(\boldsymbol{A}_r\boldsymbol{A}_r^T)^{-1}\boldsymbol{u}_r \\ & + k_N\boldsymbol{b}^T\boldsymbol{V}_N\boldsymbol{V}_N^T\boldsymbol{b}]\end{aligned} \tag{22}$$

Theorem: Consider the system described by Eqs. (7–9) with state $\boldsymbol{x} = \{\boldsymbol{\omega}, \boldsymbol{q}, q_0 - 1, \dot{\boldsymbol{\tau}}, \boldsymbol{\tau}\}$. Assume that the control laws are given by Eqs. (3), (12), (18), (20), and (22). Then, the equilibrium $\boldsymbol{x}_e = \{\boldsymbol{0}, \boldsymbol{0}, 0, \boldsymbol{0}, \boldsymbol{0}\}$ is asymptotically stable.

Proof: Consider the Lyapunov function in Eq. (10), which is a positive-definite function of the state $\boldsymbol{x}$. Using Eq. (13) with Eq. (22) yields

$$\dot{V} = -k_d\boldsymbol{\omega}^T\boldsymbol{\omega} - \dot{\boldsymbol{\tau}}^T\boldsymbol{\Xi}\dot{\boldsymbol{\tau}} - k_N\dot{\boldsymbol{\tau}}^T\boldsymbol{A}_e\boldsymbol{V}_N\boldsymbol{V}_N^T\boldsymbol{A}_e^T\dot{\boldsymbol{\tau}} \le 0 \tag{23}$$

where we have used $\boldsymbol{b} = \boldsymbol{A}_e^T\dot{\boldsymbol{\tau}}$. The invariant set contains $\boldsymbol{\omega} = \dot{\boldsymbol{\tau}} = \boldsymbol{0}$ that, when combined with the motion equations in Eqs. (7–9) and the attitude control law in Eq. (12), leads to

$$k_p\boldsymbol{q} = \boldsymbol{0}, \qquad K\boldsymbol{\tau} = \boldsymbol{0}$$

Therefore, the invariant set also contains $\boldsymbol{q} = \boldsymbol{\tau} = \boldsymbol{0}$. Given the unit length of the four-parameter quaternion, we conclude that $q_0 = \pm 1$. In a linear analysis about the equilibrium $q_0 = 1$, we can take $q_0 = 1$ in the invariant set. Hence, the invariant set consists only of the equilibrium $\boldsymbol{x}_e$, which establishes (local) asymptotic stability of the equilibrium using LaSalle's theorem.

In a singular state, all the vectors $\boldsymbol{t}_i$ of SGCMG system become coplanar and are perpendicular to a singular vector $\boldsymbol{u}_s$ [14], which satisfies $\boldsymbol{t}_i^T\boldsymbol{u}_s = 0$. A singularity measure can be applied to describing the degree of singularity, which is expressed as $\kappa = \det(\boldsymbol{A}_r\boldsymbol{A}_r^T)$, and $\kappa = 0$ indicates that the system is caught in a singular state. To reduce the impact of singularity, Eq. (20) is modified by the GSR steering law [15], which can be expressed by

$$\dot{\boldsymbol{\delta}}_r = \boldsymbol{A}_r^T(\boldsymbol{A}_r\boldsymbol{A}_r^T + \gamma\boldsymbol{E})^{-1}\boldsymbol{u}_r \tag{24}$$

where $\gamma = \gamma_1\exp[-\gamma_2\det(\boldsymbol{A}_r\boldsymbol{A}_r^T)]$, γ_1 and γ_2 are positive scalars, and E is a symmetric matrix expressed as

$$\boldsymbol{E} = \begin{bmatrix} 1 & \epsilon_3 & \epsilon_2 \\ \epsilon_3 & 1 & \epsilon_1 \\ \epsilon_2 & \epsilon_1 & 1 \end{bmatrix} \tag{25}$$

where $\epsilon_i = \epsilon_0\sin(k_\epsilon t + \phi_i)$, $i = 1, 2, 3$; and ϵ_0, k_ϵ, and ϕ_i are constant scalars to be properly selected.

In addition, there is a computational problem in Eq. (22) when $\boldsymbol{b}^T\boldsymbol{V}_N\boldsymbol{V}_N^T\boldsymbol{b} = 0$, which can be solved by adding a small positive scalar ε. Therefore, the modified steering law can be expressed as

$$\begin{aligned}\dot{\boldsymbol{\delta}} = {}& \boldsymbol{A}_r^T(\boldsymbol{A}_r\boldsymbol{A}_r^T + \gamma\boldsymbol{E})^{-1}\boldsymbol{u}_r - \boldsymbol{V}_N\boldsymbol{V}_N^T\boldsymbol{b}(\boldsymbol{b}^T\boldsymbol{V}_N\boldsymbol{V}_N^T\boldsymbol{b} + \varepsilon)^{-1} \\ & \times[\boldsymbol{b}^T\boldsymbol{A}_r^T(\boldsymbol{A}_r\boldsymbol{A}_r^T + \gamma\boldsymbol{E})^{-1}\boldsymbol{u}_r + k_N\boldsymbol{b}^T\boldsymbol{V}_N\boldsymbol{V}_N^T\boldsymbol{b}]\end{aligned} \tag{26}$$

Remark 1: The proposed steering law in Eq. (26) works without as many SGCMGs as the considered vibration modes. In particular, four SGCMGs can satisfy the requirement, which is much more feasible than the methods in other papers [12,13]. Because the truncated model with several low-frequency modes is not used in the controller and steering law design, and the rotational rates $\dot{\boldsymbol{\beta}}_i$ are the integrated results of all the modes, the method proposed in this Note is also effective in dealing with the unconsidered residual modes of vibration.

V. Modal Analysis

In this section, a modal analysis is applied to the system with consideration of the proposed method to verify its effectiveness on vibration suppression. Considering the controller in Eq. (12) and the steering law in Eq. (22), Eq. (5) can be rewritten as

$$\begin{aligned}&\begin{bmatrix} \boldsymbol{J} & \boldsymbol{M} \\ \boldsymbol{M}^T & \boldsymbol{I} \end{bmatrix}\begin{bmatrix} \dot{\boldsymbol{\omega}} \\ \ddot{\boldsymbol{\tau}} \end{bmatrix} + \begin{bmatrix} \boldsymbol{G}_{rr} + k_d\boldsymbol{I} & \boldsymbol{G}_{re} \\ -\boldsymbol{G}_{re}^T & \boldsymbol{G}_{ee} + \boldsymbol{D} \end{bmatrix}\begin{bmatrix} \boldsymbol{\omega} \\ \dot{\boldsymbol{\tau}} \end{bmatrix} \\ &\quad + \begin{bmatrix} \frac{1}{2}k_p\boldsymbol{I} & \boldsymbol{0} \\ \boldsymbol{0} & \boldsymbol{K} \end{bmatrix}\begin{bmatrix} \boldsymbol{\theta} \\ \boldsymbol{\tau} \end{bmatrix} = \boldsymbol{0}\end{aligned} \tag{27}$$

where $\boldsymbol{D} = \boldsymbol{\Xi} + k_n\boldsymbol{A}_e\boldsymbol{V}_N\boldsymbol{V}_N^T\boldsymbol{A}_e^T$ represents the lumped damping matrix on account of the control method presented in this Note and the structural damping. A small angular rotation has been assumed so that $\boldsymbol{\omega} = \dot{\boldsymbol{\theta}}$ and $\boldsymbol{q} \doteq \boldsymbol{\theta}/2$. Rewriting Eq. (27), it follows that

$$\bar{\boldsymbol{M}}\ddot{\boldsymbol{p}} + (\bar{\boldsymbol{G}} + \bar{\boldsymbol{D}})\dot{\boldsymbol{p}} + \tilde{\boldsymbol{K}}\boldsymbol{p} = \boldsymbol{0} \tag{28}$$

where

$$\bar{\boldsymbol{D}} = \begin{bmatrix} k_d\boldsymbol{I} & \boldsymbol{0} \\ \boldsymbol{0} & \boldsymbol{D} \end{bmatrix}, \qquad \tilde{\boldsymbol{K}} = \begin{bmatrix} \frac{1}{2}k_p\boldsymbol{I} & \boldsymbol{0} \\ \boldsymbol{0} & \boldsymbol{K} \end{bmatrix} \tag{29}$$

Because the SGCMGs are mounted on the elastic structure, this system is referred to as a gyroelastic body [5,6]. The equation of an undamped gyroelastic body in a first-order form can be expressed as

$$\boldsymbol{W}\dot{\boldsymbol{X}} + \boldsymbol{N}\boldsymbol{X} = \boldsymbol{0} \tag{30}$$

where

$$\boldsymbol{X} = \begin{bmatrix} \dot{\boldsymbol{p}} \\ \boldsymbol{p} \end{bmatrix}, \qquad \boldsymbol{W} = \begin{bmatrix} \bar{\boldsymbol{M}} & \boldsymbol{0} \\ \boldsymbol{0} & \tilde{\boldsymbol{K}} \end{bmatrix}, \qquad \boldsymbol{N} = \begin{bmatrix} \bar{\boldsymbol{G}} & \tilde{\boldsymbol{K}} \\ -\tilde{\boldsymbol{K}} & \boldsymbol{0} \end{bmatrix} \tag{31}$$

Clearly, $\boldsymbol{W}$ is positive definite and $\boldsymbol{N}$ is skew symmetric. The eigenvalue problem of the undamped gyroelastic system can be expressed as

$$\lambda_\alpha\boldsymbol{W}\boldsymbol{\chi}_\alpha + \boldsymbol{N}\boldsymbol{\chi}_\alpha = \boldsymbol{0}, \quad \alpha = \pm 1, \quad \pm 2, \ldots, \pm(m+3) \tag{32}$$

Table 1 System properties

Property	Symbol (unit of measure)	Value
Moment of inertia of spacecraft	$\boldsymbol{J}$ ($\mathrm{kg \cdot m^2}$)	diag (1646.3, 1924.7, 2678.3)
Moment of inertia of SGCMG	$\boldsymbol{J}_{\mathrm{cmg}}$ ($\mathrm{kg \cdot m^2}$)	diag (1.1, 2, 1.2)
Angular momentum magnitude of SGCMG	h_0 ($\mathrm{kg \cdot m^2/s}$)	100
Size	$l_1 \times l_2$ (m)	6×10
Structure damping	ξ (—)	0.01
Initial quaternion	$[q_0 \quad \boldsymbol{q}^T]^T$	$[-0.4386 \quad -0.4821 \quad -0.5576 \quad 0.5140]^T$
Initial gimbal angles	$\boldsymbol{\delta}_0$ (deg)	$[56.1 \quad -56.1 \quad 116.2 \quad -116.2]^T$
Maximum of the gimbal rates	$\dot{\delta}_{\max}$ (deg /s)	20

Table 2 Installation properties

Number	Placement coordinates	Gimbal axes $\boldsymbol{g}_i$
1	(3, −5)	$[(\sqrt{6}/3) \quad 0 \quad (\sqrt{3}/3)]^T$
2	(3, 5)	$[0 \quad (\sqrt{6}/3) \quad (\sqrt{3}/3)]^T$
3	(−3, 5)	$[-(\sqrt{6}/3) \quad 0 \quad (\sqrt{3}/3)]^T$
4	(−3, −5)	$[0 \quad -(\sqrt{6}/3) \quad (\sqrt{3}/3)]^T$

where $\lambda_\alpha = j\Omega_\alpha$ denotes the αth eigenvalue, and $\boldsymbol{\chi}_\alpha = \boldsymbol{\phi}_\alpha + j\boldsymbol{\varphi}_\alpha$ denotes the αth eigenvector. The vectors $\boldsymbol{\phi}_\alpha$ and $\boldsymbol{\varphi}_\alpha$ are real matrices satisfying $\boldsymbol{\phi}_\alpha = \boldsymbol{\varphi}_{-\alpha}$, and they can be expressed as

$$\boldsymbol{\phi}_\alpha = \begin{bmatrix} -\Omega_\alpha \boldsymbol{\nu}_\alpha \\ \boldsymbol{\mu}_\alpha \end{bmatrix}, \qquad \boldsymbol{\varphi}_\alpha = \begin{bmatrix} \Omega_\alpha \boldsymbol{\mu}_\alpha \\ \boldsymbol{\nu}_\alpha \end{bmatrix} \tag{33}$$

where $\boldsymbol{\mu}_\alpha = \boldsymbol{\nu}_{-\alpha}, \boldsymbol{\mu}_{-\alpha} = \boldsymbol{\nu}_\alpha$; and $(\boldsymbol{\mu}_\alpha, \boldsymbol{\nu}_\alpha)$ are referred to as gyroelastic modes [5,6]. The following orthogonality conditions are satisfied:

$$\begin{aligned} \boldsymbol{\phi}_\alpha^T \boldsymbol{W} \boldsymbol{\phi}_\beta &= \boldsymbol{\varphi}_\alpha^T \boldsymbol{W} \boldsymbol{\varphi}_\beta = 2\Omega_\alpha^2 \delta_{\alpha\beta} \\ \boldsymbol{\phi}_\alpha^T \boldsymbol{N} \boldsymbol{\varphi}_\beta &= -2\Omega_\alpha^3 \delta_{\alpha\beta} \end{aligned} \tag{34}$$

where $\delta_{\alpha\beta}$ denotes the Kronecker delta symbol.

In view of the light damping assumption, the damping is treated as a perturbation to the undamped gyroelastic system [17], leading to perturbed quantities as follows:

$$\begin{aligned} \bar{\lambda}_\alpha &= \lambda_\alpha + \delta\lambda_\alpha \\ \bar{\boldsymbol{\phi}}_\alpha &= \boldsymbol{\phi}_\alpha + \delta\boldsymbol{\phi}_\alpha \\ \bar{\boldsymbol{\varphi}}_\alpha &= \boldsymbol{\varphi}_\alpha - \delta\boldsymbol{\phi}_\alpha \end{aligned} \tag{35}$$

where $\delta\lambda_\alpha = \varsigma_\alpha \Omega_\alpha$, and ς_α represents the αth damping factor that, for small damping, can be expressed as

$$\varsigma_\alpha = \frac{1}{4\Omega_\alpha} (\boldsymbol{\mu}_\alpha^T \bar{\boldsymbol{D}} \boldsymbol{\mu}_\alpha + \boldsymbol{\nu}_\alpha^T \bar{\boldsymbol{D}} \boldsymbol{\nu}_\alpha) \tag{36}$$

In the present context, $\boldsymbol{D}$ is given in Eq. (29) with $\boldsymbol{D} = \boldsymbol{\Xi} + k_n \boldsymbol{A}_e \boldsymbol{V}_N \boldsymbol{V}_N^T \boldsymbol{A}_e^T$. Therefore, the damping factors are increased due to the null motion. The vector $\delta\boldsymbol{\phi}_\alpha$ can be expanded in terms of the unperturbed eigenfunctions as follows:

$$\delta\boldsymbol{\phi}_\alpha = \sum_{i=-m-3}^{m+3} c_{\alpha,i} \boldsymbol{\phi}_\alpha \tag{37}$$

where

$$\begin{aligned} c_{\alpha,i} &= \frac{\Omega_\alpha \Omega_i \rho_{-\alpha,i} - \Omega_\alpha^2 \rho_{\alpha,-i}}{2\Omega_i (\Omega_i^2 - \Omega_\alpha^2)}, \quad i \neq \pm\alpha \\ c_{\alpha,\alpha} &= -\frac{\rho_{\alpha,-\alpha}}{4\Omega_\alpha}, \quad c_{\alpha,-\alpha} = -\frac{\rho_{-\alpha,-\alpha} - \rho_{\alpha,\alpha}}{8\Omega_\alpha} \end{aligned} \tag{38}$$

and $\rho_{\alpha,i} = \boldsymbol{\mu}_\alpha^T \bar{\boldsymbol{D}} \boldsymbol{\mu}_i$. The orthogonality conditions are similar to Eq. (34) as follows:

$$\begin{aligned} \bar{\boldsymbol{\phi}}_\alpha^T \boldsymbol{W} \bar{\boldsymbol{\phi}}_\beta &= \bar{\boldsymbol{\varphi}}_\alpha^T \boldsymbol{W} \bar{\boldsymbol{\varphi}}_\beta = 2\Omega_\alpha^2 \delta_{\alpha\beta} \\ \bar{\boldsymbol{\phi}}_\alpha^T \boldsymbol{N} \bar{\boldsymbol{\varphi}}_\beta &= 2\Omega_\alpha^3 (\varsigma_\alpha \delta_{\alpha\beta} - \delta_{-\alpha\beta}) \end{aligned} \tag{39}$$

The general solutions of Eq. (30) can be written as

$$\boldsymbol{X}(t) = \sum_{\alpha=-m-3}^{m+3} \bar{\boldsymbol{\phi}}_\alpha \eta_\alpha(t), \quad \alpha \neq 0 \tag{40}$$

where $\eta_\alpha(t)$ denotes a generalized coordinate.

Then, the state-space model of the gyroelastic system with consideration of both proportional and derivative terms of the proposed controller can be written as

$$\begin{bmatrix} \dot{\eta}_1 \\ \dot{\eta}_{-1} \\ \vdots \\ \dot{\eta}_{m+3} \\ \dot{\eta}_{-m-3} \end{bmatrix} = \begin{bmatrix} -\varsigma_1\Omega_1 & \Omega_1 & \cdots & & \mathbf{0} & \\ -\Omega_1 & -\varsigma_1\Omega_1 & & & & \\ & \vdots & \ddots & & \vdots & \\ & & & -\varsigma_{m+3}\Omega_{m+3} & & \Omega_{m+3} \\ & \mathbf{0} & \cdots & -\Omega_{m+3} & & -\varsigma_{m+3}\Omega_{m+3} \end{bmatrix} \times \begin{bmatrix} \eta_1 \\ \eta_{-1} \\ \vdots \\ \eta_{m+3} \\ \eta_{-m-3} \end{bmatrix} \tag{41}$$

which illustrates that the rate of convergence is dependent on the damping factors ς_α.

Remark 2: Because of the null motion, the damping factors are increased, which will make the elastic motion be damped out more

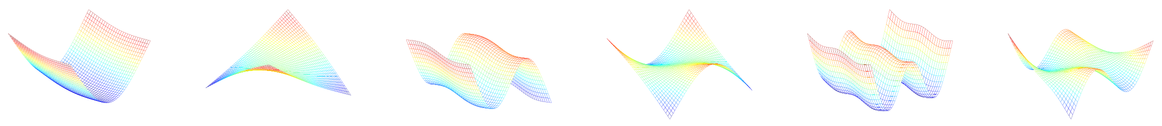

a) ω_1 = 0.7681 Hz b) ω_2 = 1.1038 Hz c) ω_3 = 1.8733 Hz d) ω_4 = 2.5496 Hz e) ω_5 = 3.1438 Hz f) ω_6 = 3.592 Hz

Fig. 2 Free plate elastic modes.

Table 3 Controller and steering law parameters

Symbol	Value
k_p	60
k_d	400
γ_1	0.01
γ_2	10
ϵ_0	0.021
k_ϵ	0.5
φ_1	0
φ_2	$\pi/2$
φ_3	π
k_N	0.1
ε	0.000001

quickly. Although the damping factors are increased a little bit, they have a major effect on the vibration. More important, the possible undesirable effects of the modal forces on the elastic dynamics are eliminated by the proposed method.

VI. Simulation

The properties of the considered unconstrained flexible spacecraft are shown in Table 1. Four SGCMGs making up a pyramid type are mounted on the four corners of the equivalent plate to realize the desired attitude maneuver and vibration suppression. As shown in Fig. 2, six constrained modes of the structure are considered. Although scaled here for visualization purposes, they are normalized to unity with respect to the mass distribution. The skew angle of the pyramid-type SGCMG system is equal to 54.73 deg, and the installation properties are given in Table 2.

The external disturbances are assumed to be

$$\boldsymbol{T}_d = \begin{bmatrix} 0.4\cos(0.1t) - 0.1 \\ 0.25\sin(0.1t) + 0.4\cos(0.1t) \\ 0.4\sin(0.1t) + 0.1 \end{bmatrix} \text{N}\cdot\text{m} \tag{42}$$

For comparison, the attitude controller in Eq. (12) and the steering law in Eq. (24) without null motion are used in case I, and the proposed method in this Note is applied to case II. The parameters of the controller and steering law can be found in Table 3.

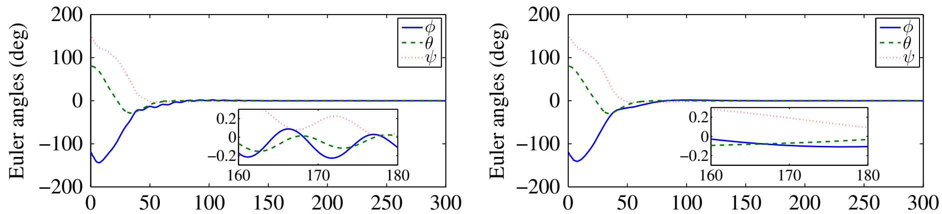

a) Case I b) Case II

Fig. 3 Time histories of Euler angles.

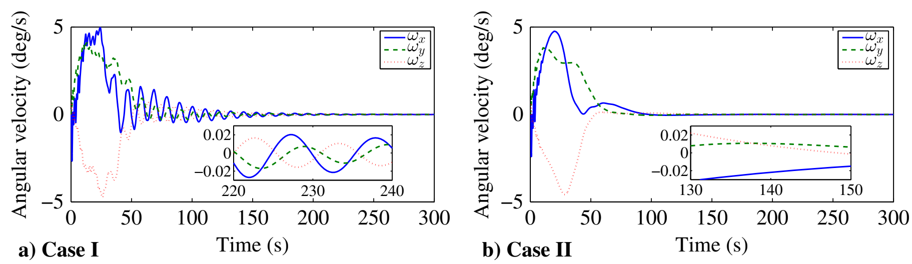

a) Case I b) Case II

Fig. 4 Time histories of angular velocity.

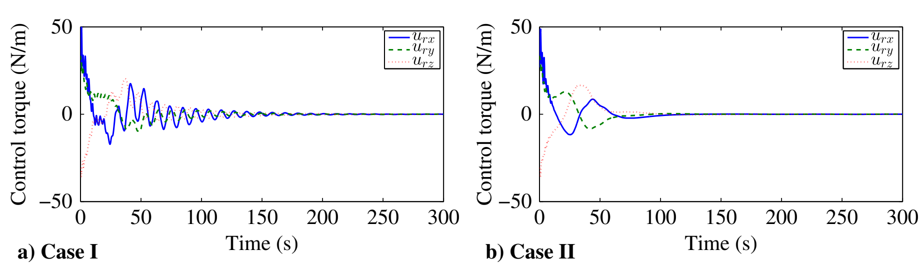

a) Case I b) Case II

Fig. 5 Time histories of control torque.

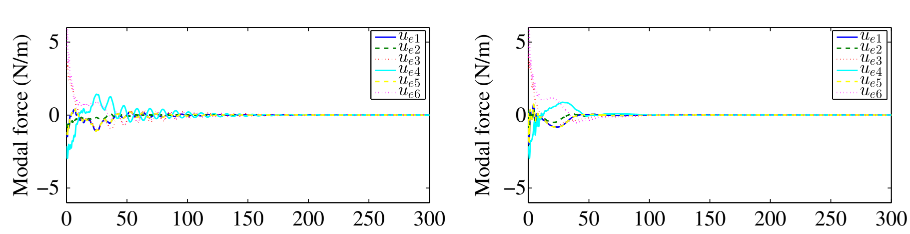

a) Case I b) Case II

Fig. 6 Time histories of modal force.

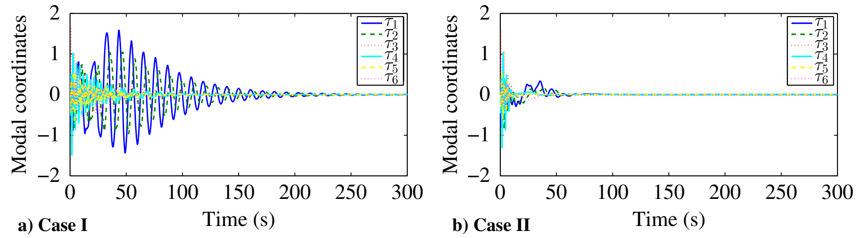

Fig. 7 Time histories of modal coordinates.

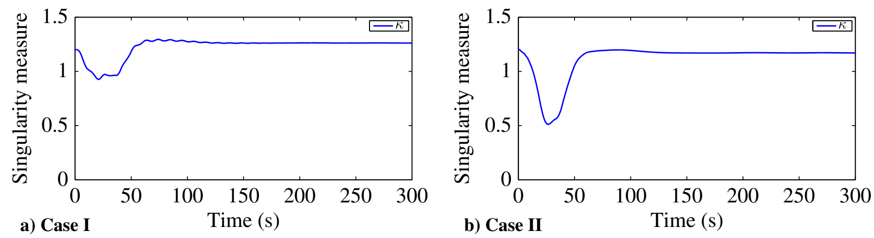

Fig. 8 Time histories of singularity measure.

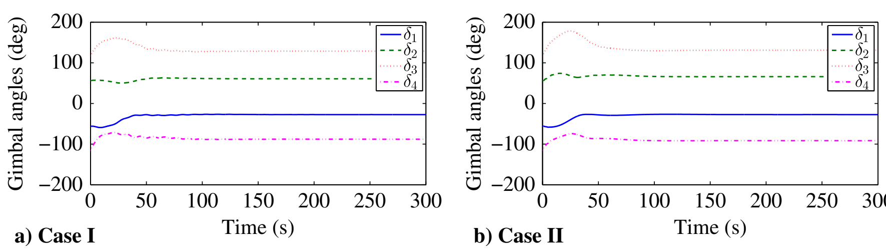

Fig. 9 Time histories of gimbal angles of SGCMGs.

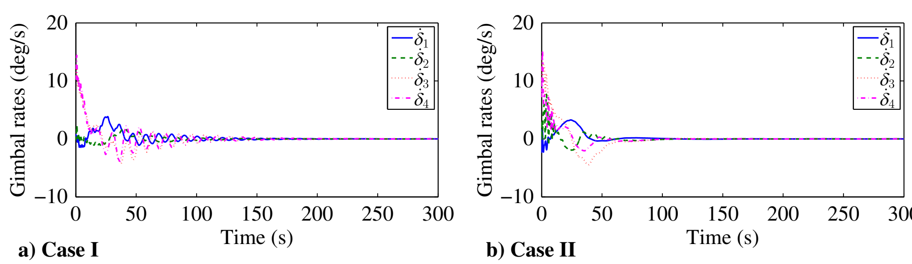

Fig. 10 Time histories of gimbal rates of SGCMGs.

Figures 3 and 4 show the time histories of the Euler angles (ψ, θ, and ϕ correspond to a 3-2-1 sequence) and the angular velocity, respectively. Considering the allowable attitude pointing accuracy and attitude stability are within 0.2 deg and 0.02 deg /s, respectively, the attitude maneuver times (i.e., the time to obtain the desired limits) are 233.3 and 169.1 s, respectively. When compared with case I, the system is much quicker to become stable on account of the damping added by null motion in case II. The time histories of the control torques and modal forces are shown in Figs. 5 and 6, respectively. Figure 7 shows the time histories of the modal coordinates, which illustrate that vibration is effectively suppressed by the proposed method. The time histories of the singularity measure are shown in Fig. 8, which illustrates that the system is not caught in a singular state during the attitude maneuver. Figures 9 and 10 show the time histories of the gimbal angles and gimbal rates, respectively, which meet the requirements in Table 1. All of these figures illustrate that the singularity modifications [γ and ϵ in Eq. (26)] do not result in graphically discernible residual motions.

In Ref. [13], a structure with identical mass and stiffness properties was employed with an identical attitude maneuver under study. The external disturbance torques were slightly different, but they were of the same order of magnitude as those used here. In that study [13], eight SGCMGs were used for vibration control and additional torque actuation was required for attitude control. The attitude performance was somewhat faster in Ref. [13] (settling times for the Euler angles were on the order of 20 s as compared to approximately 50 s in the present work. This can be attributed to larger attitude control gains in Ref. [13]). In the present work, the modal coordinates in Fig. 7b are on the order of one, whereas in Ref. [13], they were on the order of 10^{-4} (see figure 14 in Ref. [13]). Hence, the use of additional SGCMGs dedicated to vibration control in Ref. [13] provided more effective vibration suppression than the current approach. However, in the present work, four SGCMGs are solving the attitude control problem and vibration control of all controllable modes.

VII. Conclusions

A new methodology for flexible spacecraft that realizes attitude maneuvers and vibration suppression has been proposed in the Note. A set of single-gimbaled control moment gyroscopes (SGCMGs) was mounted on the elastic structure as actuators to generate net control torques and modal forces. A simple controller based on a Lyapunov function and a generalized singular robust steering law have been presented. To suppress the vibration, proper null motion has been added to the steering law to eliminate the possible undesirable effects of modal forces on the elastic dynamics. The proposed method works without as many SGCMGs as the vibration modes, and four SGCMGs can be effective in dealing with all the considered modes. A modal analysis on the system with consideration of the proposed method illustrates that the damping is increased and the system becomes stable more quickly. Furthermore, the proposed control strategies have been applied to an unconstrained flexible plate with four SGCMGs mounted on the corners. The simulation results have verified the effectiveness of the proposed method for vibration suppression during attitude maneuvers.

Acknowledgment

The work reported in this Note is partially supported by the China Scholarship Council.

References

[1] Gennaro, S., "Active Vibration Suppression in Flexible Spacecraft Attitude Tracking," *Journal of Guidance, Control, and Dynamics*, Vol. 21, No. 3, 1998, pp. 400–408. doi:10.2514/2.4272

[2] Gennaro, S., "Output Attitude Tracking for Flexible Spacecraft," *Automatica*, Vol. 38, No. 10, 2002, pp. 1719–1726. doi:10.1016/S0005-1098(02)00082-1

[3] Gennaro, S., "Output Stabilization of Flexible Spacecraft with Active Vibration Suppression," *IEEE Transactions on Aerospace and Electronic Systems*, Vol. 39, No. 3, 2003, pp. 747–759. doi:10.1109/TAES.2003.1238733

[4] Hu, Q., Jia, Y., and Xu, S., "Adaptive Suppression of Linear Structural Vibration Using Control Moment Gyroscopes," *Journal of Guidance, Control, and Dynamics*, Vol. 37, No. 3, 2014, pp. 990–996. doi:10.2514/1.62267

[5] D'Eleuterio, G., and Hughes, P., "Dynamics of Gyroelastic Continua," *Journal of Applied Mechanics*, Vol. 51, No. 2, 1984, pp. 415–422. doi:10.1115/1.3167634

[6] D'Eleuterio, G., and Hughes, P., "Dynamics of Gyroelastic Spacecraft," *Journal of Guidance, Control, and Dynamics*, Vol. 10, No. 4, 1987, pp. 401–405. doi:10.2514/3.20231

[7] Yang, L. F., Mikulas, M. M., Jr., and Park, K., "Slewing Maneuvers and Vibration Control of Space Structures by Feedforward/Feedback Moment-Gyro Controls," *Journal of Dynamic Systems, Measurement, and Control*, Vol. 117, No. 3, 1995, pp. 343–351. doi:10.1115/1.2799125

[8] Shi, J., and Damaren, C., "Control Law for Active Structural Damping Using a Control Moment Gyro," *Journal of Guidance, Control, and Dynamics*, Vol. 28, No. 3, 2005, pp. 550–553. doi:10.2514/1.11269

[9] Chee, S., and Damaren, C., "Optimal Gyricity Distribution for Space Structure Vibration Control," *Journal of Guidance, Control, and Dynamics*, Vol. 38, No. 7, 2014, pp. 1218–1228. doi:10.2514/1.G000293

[10] Jia, S., Jia, Y., Xu, S., and Hu, Q., "Optimal Placement of Sensors and Actuators for Gyroelastic Body Using Genetic Algorithms," *AIAA Journal*, Vol. 54, No. 8, 2016, pp. 2472–2488. doi:10.2514/1.J054696

[11] Jia, S., and Shan, J., "Optimal Actuator Placement for Constrained Gyroelastic Beam Considering Control Spillover," *Journal of Guidance, Control, and Dynamics*, Vol. 41, No. 9, 2018, pp. 2073–2081. doi:10.2514/1.G003560

[12] Hu, Q., and Zhang, J., "Attitude Control and Vibration Suppression for Flexible Spacecraft Using Control Moment Gyroscopes," *Journal of Aerospace Engineering*, Vol. 29, No. 1, 2015, Paper 04015027. doi:10.1061/(ASCE)AS.1943-5525.0000513

[13] Guo, J., Geng, Y., Wu, B., and Kong, X., "Vibration Suppression of Flexible Spacecraft During Attitude Maneuver Using CMGs," *Aerospace Science and Technology*, Vol. 72, No. 1, 2018, pp. 183–192. doi:10.1016/j.ast.2017.11.005

[14] Margulies, G., and Aubrun, J., "Geometric Theory of Single-Gimbal Control Moment Gyro System," *Journal of Astronautical Sciences*, Vol. 26, No. 2, 1978, pp. 159–191.

[15] Wie, B., "Singularity Escape/Avoidance Steering Logic for Control Moment Gyro Systems," *Journal of Guidance, Control, and Dynamics*, Vol. 28, No. 5, 2005, pp. 948–956. doi:10.2514/1.10136

[16] Hu, Q., Guo, C., and Zhang, J., "Singularity and Steering Logic for Control Moment Gyros on Flexible Space Structures," *Acta Astronautica*, Vol. 137, Aug. 2017, pp. 261–273. doi:10.1016/j.actaastro.2017.04.030

[17] Damaren, C., and D'Eleuterio, G., "Optimal Control of Large Space Structures Using Distributed Gyricity," *Journal of Guidance, Control, and Dynamics*, Vol. 12, No. 5, 1989, pp. 723–731. doi:10.2514/3.20467